Bound exciton effect and carrier escape mechanisms in temperature-dependent surface photovoltage spectroscopy of a single quantum well

Shouvik Datta,[1,*] B. M. Arora,[1] and Shailendra Kumar[2]
[1]Department of Condensed Matter Physics and Materials Science, Tata Institute of Fundamental Research, Homi Bhabha Road, Mumbai–400 005, India
[2]Center for Advanced Technology, Indore–452 013, India
(Received 8 May 2000)

The temperature dependence of the surface photovoltage spectrum of a strained GaAs/$In_xGa_{1-x}As$/GaAs single quantum well shows unusual broadening of the line shape around the e_1-hh_1 feature below 100 K. With evidence obtained from the temperature dependence of the photoluminescence spectrum, this unusual broadening is attributed to a bound exciton transition that is prominent at low temperatures. Selectively excited dc photocurrent experiments show that thermal emission and field-aided tunneling emission of photogenerated carriers from the quantum well are responsible for the charge separation and subsequent generation of surface photovoltage of the quantum well.

I. INTRODUCTION

Surface photovoltage spectroscopy (SPS) is a well-known technique to map the electronic structure of bulk semiconductors near the band edge as well as at sub-band-gap energies. In surface photovoltage[1–8] (SPV) experiments we measure the change in surface potential due to optically excited electron-hole pair generation under periodic illumination and subsequent carrier redistribution and/or capture in the surface states. Recently, SPV measurement has emerged as a powerful technique[9] to study surface states,[10–15] heterojunctions,[16,17] quantum wells (QWs),[18–20] and other nanostructures.[21–23]

In this paper we report SPS experiments on a single-QW structure of strained GaAs/$In_xGa_{1-x}As$/GaAs over a wide range of temperatures from 300 to 8 K. The results show an unexpected increase in peak width around the e_1-hh_1 feature in the SPV spectrum below 100 K. From comparison of the temperature dependence of SPV and photoluminescence (PL) spectra, we attribute the broadening to a bound exciton transition that is significant at low temperatures. We also report selectively excited dc photocurrent experiments on the QW structure using a top Au Schottky contact with bias and temperature dependence and show that both thermal emission and field-aided tunneling emission of photogenerated carriers are responsible for the SPV.

II. EXPERIMENTAL ARRANGEMENT

SPS, electroreflectance (ER),[24–26] and PL (Ref. 27) measurements were done on strained GaAs/$In_xGa_{1-x}As$/GaAs single-quantum-well samples (with nominal In content $x \approx 0.2$) grown in our laboratory by using metal-organic vapor-phase epitaxy. The SPV measurement is done with chopped light in a capacitive geometry in a vacuum jig ($<10^{-4}$ mbar) at various temperatures from 300 to 8 K (with $\Delta T \sim \pm 1$ K) using a closed-cycle He refrigerator and a temperature controller. The sample is mounted on an L-shaped copper plate with silver epoxy and attached to the cold finger of the cold head which acts as the ground electrode. A transparent conducting glass plate (coated with indium tin oxide or ITO on the surface facing the sample) is used as the top electrode as well as the window for the light to shine on the sample. The ITO-coated surface of the glass window is adjusted to gently touch the top surface of the sample. Experimental details of touching the sample surface will be discussed in detail in a separate paper.[28] A 150 W quartz-tungsten-halogen lamp along with a $\frac{1}{8}$ Oriel monochromator (77250) having a grating with 1000 nm blaze wavelength (128 Å/mm dispersion) is used as the light source. The spectral bandpass is kept at approximately 30 Å to optimize the balance between the resolution and the signal strength. Light from the monochromator is chopped at a frequency of 20 ± 0.1 Hz before being focused on the sample through the top transparent electrode. The ac photovoltage is picked up by the ITO-coated transparent electrode, using a unity gain buffer circuit and measured with an SR830 lock-in amplifier. A 715 nm order sorting filter is used to block unwanted higher-order lines from the monochromator. λ^2 correction is applied to the measured SPV spectrum to represent it as a function of energy. In the region of the QW spectrum, the measured spectral response of the excitation light from the lamp and monochromator combination is found to be nearly independent of wavelength, thus requiring no further correction for excitation intensity normalization.[21] In all SPS measurements, we scan from a wavelength 750 nm, well above the GaAs band edge, to 1100 nm, below the band gap of InGaAs.

The experimental arrangement for the ER measurement is standard[24–26] except for the fact that the top conducting transparent ITO electrode gently touches the sample surface.[28] A Ge detector is used to measure the reflected light. For PL experiments we use a model 207 McPherson 0.67 meter scanning monochromator with a 488 nm Ar^+ laser as the excitation and a Si diode as the detector.

III. CHARACTERIZATION OF SINGLE QW USING SPV AND ER SPECTRA

Figure 1(a) shows the room-temperature SPV spectrum for a nominal 70 Å strained QW structure (sample A) of

 ©2000 The American Physical Society

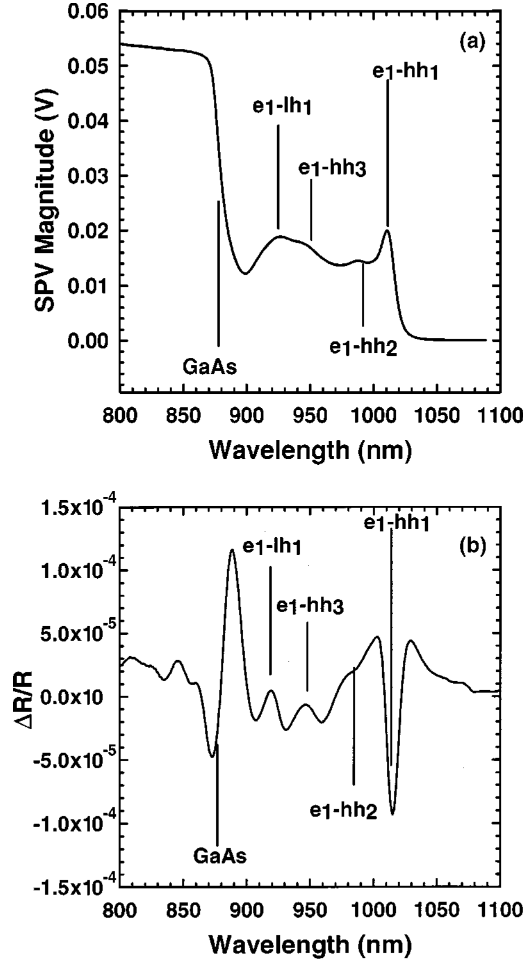

FIG. 1. (a) SPV spectrum of sample A at room temperature; (b) corresponding ER spectrum of sample A at room temperature.

TABLE I. Comparison of transition energy values (in eV) as calculated for a strained GaAs/$In_{0.23}Ga_{0.77}As$/GaAs single quantum well and the values determined from SPV and ER spectra. e_1-hh_1, e_1-lh_1, GaAs transition energies of SPV and e_1-hh_1, GaAs transition energies of ER are obtained by fitting an Aspnes line shape [Eq. (1)] with appropriate values of m. The rest of the transition energies are directly located from the respective spectra without any fitting.

	e_1-hh_1	e_1-hh_2	e_1-hh_3	e_1-lh_1	GaAs
SPV	1.224	1.255	1.306	1.344	1.416
ER	1.228	1.260	1.306	1.347	1.417
Calculated value	1.228	1.258	1.305	1.356	

GaAs/$In_xGa_{1-x}As$/GaAs with $x \approx 0.2$. The top layer thickness is 1000 Å and n-type doping is approximately $5 \times 10^{16}\,cm^{-3}$. The spectrum consists of a feature characteristic of the band edge of GaAs and several features characteristic of the transitions between conduction and valence subbands of the QW. An ER spectrum of sample A is shown in Fig. 1(b). QW transition energy values from the ER spectrum are obtained by using a numerical fit of the Aspnes[29,30] line shape function,

$$\frac{\Delta R}{R} = \tilde{\alpha}(\omega)\Delta\varepsilon_1(\omega) + \tilde{\beta}(\omega)\Delta\varepsilon_2(\omega)$$

$$\cong \sum_{j=1}^{n} \text{Re}[a_j \exp(i\theta_j)/(E - E_{0j} + i\Gamma_{0j})^m], \qquad (1)$$

where $i = \sqrt{-1}$, $\varepsilon(\omega)$ is the dielectric constant$=\varepsilon_1(\omega) + i\varepsilon_2(\omega)$, $\tilde{\alpha}(\omega)$ and $\tilde{\beta}(\omega)$ are Seraphin's coefficients, and E_{0j} and Γ_{0j} are the energy and broadening parameters of the jth transition, respectively. For $m=3$, the line shape approximately takes care of the inhomogeneous broadening within a QW. For the bulk GaAs we use the same line shape with $m=2.5$ for the third-derivative functional form with Lorentzian broadening.

In order to obtain the transition energy values from the SPV spectrum, we first numerically calculate the first-derivative spectrum $(d[EV(E)]/dE \text{ vs } E)$ of the SPV and then similarly fit the Aspnes line shape function to the resultant derivative spectrum. This forms an analytical criterion[28] for extracting the transition energies for a QW for which $\alpha t \ll 1$, where α is the absorption coefficient and t is the well width, and the SPV can be shown to be $\sim \alpha/E$. In the next section we will show that the transition energies of the GaAs band edge at various temperatures as determined by this method produce fitting parameters which are in close agreement with those in the literature. So we adopt this method for the bulk materials as an operational procedure to extract the transition energies from the SPV spectra.

The experimental values of the transition energies obtained from the SPV and ER spectra are listed in Table I. Also listed are the values calculated for a strained GaAs/$In_{0.23}Ga_{0.77}As$/GaAs single QW of width 70 Å. Close agreement is seen between the transition energy values obtained from the two spectroscopies and the calculated transition energies.

IV. TEMPERATURE DEPENDENCE OF SPV SPECTRUM AND BOUND EXCITON EFFECT

Figure 2 shows the SPV spectra of sample B (100 Å QW of GaAs/$In_{0.26}Ga_{0.74}As$/GaAs) at several temperatures over the range 150 to 27 K. The transition energies obtained by the procedure outlined above for the GaAs band edge and e_1-hh_1 transitions are plotted in Fig. 3. As expected, the spectra shift to higher energies with lower sample temperature. Although it is not the main thrust of this paper, we shall briefly comment on the above results since the temperature dependence of the transition energies of bulk semiconductors and their quantum structures is a topic of considerable interest.[31–39] We have tried to fit our experimental results into different equations available in the literature, namely, (i) the empirical relation of Varshni,[31] (ii) two different equations of Passler,[32] considering different expressions for the electron-phonon interactions, and (iii) an equation of Vina, Logothetidis, and Cardona[33] based on similar considerations. Results of fits to these equations are presented in Table II. Although there is considerable scatter, in general we find a feature common to all these fittings, in that the values of the parameter β or Θ, characteristic of the average phonon energy, are found to be smaller for the InGaAs QW than for GaAs. We also conclude that, since the values of the parameters obtained for GaAs are in close agreement with those in

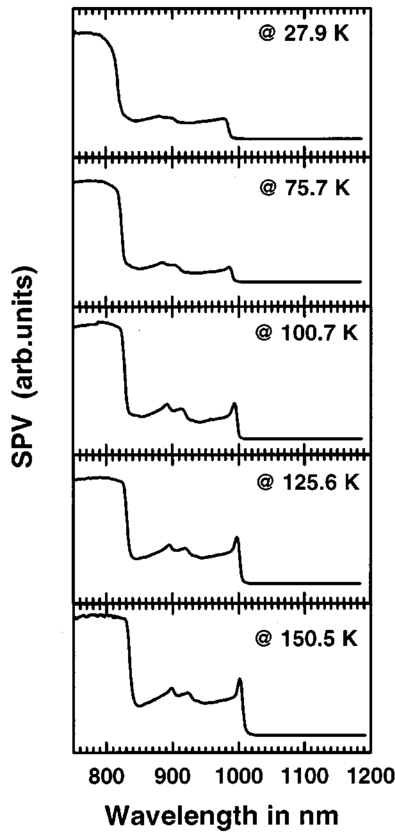

FIG. 2. SPV spectrum of sample B at different temperatures. Loss of sharpness of the e_1-hh_1 transition is obvious below 100 K. Figures are not to scale.

the literature (case 3 in Table II), the method of extracting the band-gap energy of the bulk materials from the SPV spectra as described in the previous section is a fairly good operational procedure.

A surprising feature of the temperature-dependent spectra in Fig. 2 is the shape near the e_1-hh_1 transition as the sample

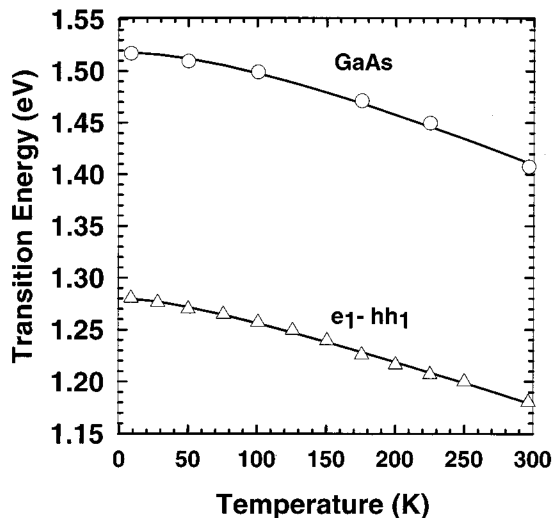

FIG. 3. Energies of various transitions as obtained from the SPV spectrum of Fig. 2 plotted against temperature. Continuous line represent the values of those transitions at various temperatures as fitted with Varshni's equation. Fitting parameters are shown in Table II (cases 2 and 3).

temperature is lowered below 100 K. There is an obvious loss of sharpness at lower temperatures. Figure 4 shows the plot of the broadening parameter (Γ_0) of the e_1-hh_1 transition vs temperature obtained by fitting the line shape to the numerical derivative spectra of the SPV at various temperatures as mentioned above. From the plot we see that after an initial decrease from room temperature the broadening parameter for the e_1-hh_1 transition is nearly constant up to $\sim$100 K and then begins to increase as the temperature is decreased. The same features are also observed from measurements on sample A. However, the Γ_0 values for the GaAs transition decrease monotonically with temperature (see the inset of Fig. 4). As such the Γ_0 values of the QW are large and symptomatic of inhomogeneous broadening induced by the quality of our QW material/structure. Even so the increase of Γ_0 at lower temperatures is unexpected. It may be remarked that broadening of the spectral features at low temperatures is also observable but overlooked in the SPV spectra of InGaAs QW samples reported recently by Wu, Wang, and Huang.[40]

Some insight into the nature of the broadening is obtained from the photoluminescence spectra of sample A shown in Fig. 5 for temperatures between 19.7 and 101.4 K. These spectra are also broader at lower temperatures. Moreover, we can observe a prominent shoulder $P2$ on the low-energy side of the main peak $P1$ at 19.7 K. The peak $P1$ is assigned as the e_1-hh_1 transition. The shoulder $P2$ almost vanishes as the temperature is raised beyond 70 K. From this temperature-dependent behavior, we assign the shoulder to a bound exciton (BE) transition[41] since this feature shows up on the low-energy side of the e_1-hh_1 peak and vanishes as the temperature is increased. Similar PL features are also reproduced in sample B.

We have carried out deconvolution of the PL spectra, separating the peaks $P1$ and $P2$, assuming the total line shape to be double Gaussian below 101.4 K (having average peak separation of $\sim$7 meV) and single Lorentzian above 101.4 K. The integrated intensities of the deconvoluted peaks at various temperatures are plotted in Fig. 6 on a semilogarithmic Arrhenius plot as functions of 1000/T. Activation energies of quenching of the peaks $P1$ and $P2$ are obtained by fitting the plot in Fig. 6 to the equation[42,43]

$$I \approx \frac{I_0}{1+\gamma \exp(-\Delta E/kT)}. \tag{2}$$

The activation energy values obtained by the fitting are $\Delta E_{P1} = 160.2\,\text{meV}$ and $\Delta E_{P2} = 16.1\,\text{meV}$. ΔE_{P1} represents quenching of the PL from the e_1-hh_1 transition and is connected closely to the emission of charge carriers from the QW explored in the next section. ΔE_{P2}, on the other hand, represents quenching of the PL of the bound exciton due to thermal activation from the bound to the free exciton. Since the rise in the SPV broadening parameter (Γ_0) is also significant below $\sim$70 K, the temperature below which the PL shoulder $P2$ becomes significant, it is proposed that the SPV broadening is caused by the onset of the upward bound exciton transition. From the evidence presented above, the mechanism seems highly plausible. Above $\sim$70 K, the BE transition strength reduces significantly and almost vanishes

TABLE II. Values of the parameters obtained by fitting the transition energy vs temperature with different expressions given in the literature: Varshni's equation (cases 1–3), Passler equations (case 4–7), and Vina *et al.* equation (cases 8 and 9). Brief comments on the fitted results are given in the right column.

Transition	$E_G(0)$ (eV)	$10^{-4}\alpha$ (eV/K)	β or Θ (K)	a_B	ρ or P	Fitted equations and remarks
1. GaAs	1.5182±0.0020	6.05±0.2	200.0			Varshni eqn. Eq. (1) of Ref. 31. In case 1, value of β is kept constant (Ref. 34). Also see Refs. 34–36.
2. e_1-hh_1	1.2801±0.0013	4.31±0.24	81.0±21.4			
3. GaAs	1.515±0.001 28	10.81±2.75	588.9±224			Fitted with Varshni eqn. Parameters are in close agreement with Table I of Ref. 36.
4. GaAs	1.514±0.0019	6.104±0.72	282.8±55.34		$p\approx 2.5$	Passler eqn. Eq. 6 of Ref. 32. Also see Refs. 37–39. Dependence on the values of p ($2<p<3$) is weak in both cases.
5. e_1-hh_1	1.279±0.0013	4.013±0.14	104.8±17.2		$p\approx 2.5$	
6. GaAs	1.514±0.0017	6.452±0.76	483.5±91.4		$\rho\approx 0.6$	Passler eqn. Eq. (9) of Ref. 32. Also see Refs. 37–39. Dependence on the values of ρ ($0.3<\rho<1$) is weak in both cases.
7. e_1-hh_1	1.279±0.001 33	4.068±1.47	165.2±28.6		$\rho\approx 0.6$	
8. GaAs	$E_B=1.5884\pm 0.022$		265.64±55.1	0.0753±0.024		Eq. (4) of Ref. 33. $E_G(0)=E_B-a_B$. Also see Refs. 36 and 37.
9. e_1-hh_1	$E_B=1.3\pm 0.0035$		109.7±18.9	0.022±0.0044		

beyond 101.4 K, precluding observation of any broadening due to this mechanism either in PL or in the SPV.

Another question needs to be discussed regarding the shape of the SPV spectra at low temperatures. Unlike PL, why are we not able to resolve this BE transition in the SPV even though the experimental resolution is kept the same in both the PL and the SPV experiments? To understand this qualitatively, we note that the SPV signal is different from a pure absorption signal since the excitations at higher energy (say, from the e_1-hh_1 level) can decay to the BE state, which in turn can either decay radiatively by PL or dissociate and

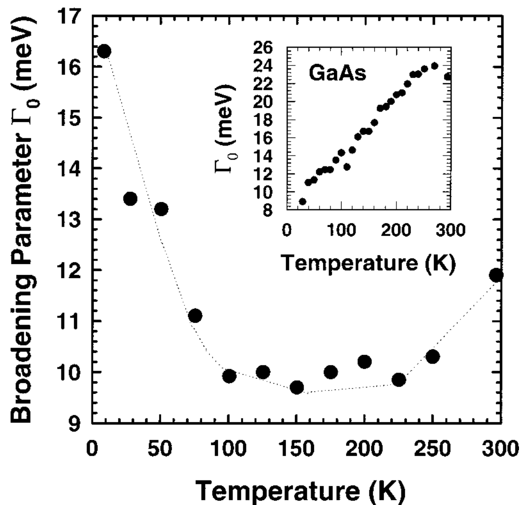

FIG. 4. The broadening parameter (Γ_0) of e_1-hh_1 as obtained from the SPV spectrum of sample B. Clearly Γ_0 increases below 100 K. Inset shows the broadening of the GaAs transition at various temperatures. The dotted line is a guide to the eye and not a fit.

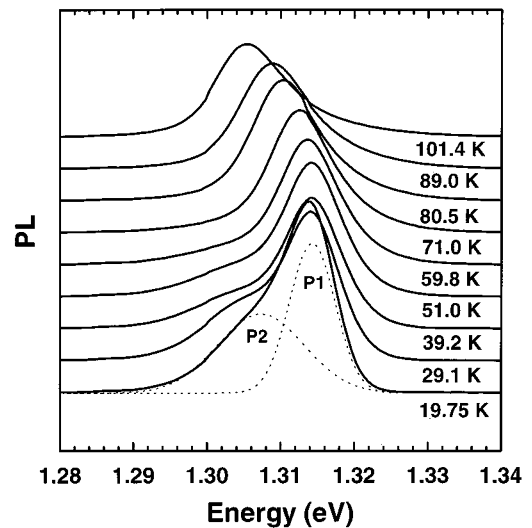

FIG. 5. Photoluminescence spectrum of sample A at various temperatures. The prominent shoulder at the low-energy side of the e_1-hh_1 transition at the lower temperatures is attributed to a bound excitonic transition. The spectra at various temperatures are shifted on the vertical scale for ease of presentation. A deconvolution of the PL spectra at the lowest temperature is also shown.

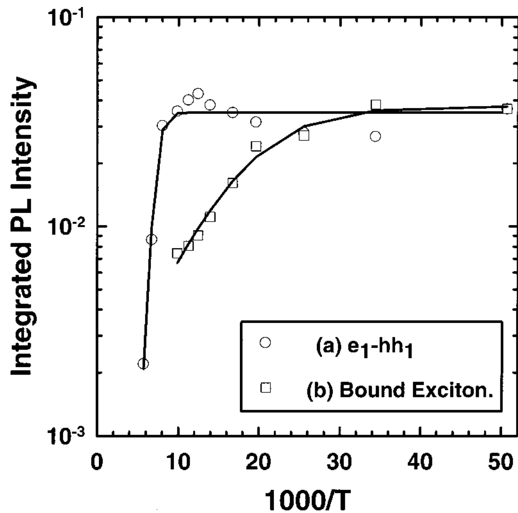

FIG. 6. PL intensities of (a) the e_1-hh$_1$ transition and (b) the bound exciton transition are plotted against 1000/T. Interestingly, the PL intensity starts saturating below 100 K.

produce SPV. Similarly, carriers from the BE level can also be excited to the e_1-hh$_1$ level and then subsequently excited to form e^--h pairs (as $\Delta E_{P2} \ll \Delta E_{P1}$) to generate SPV. Being a two-step process, the probability of SPV generation from the BE level may be small compared to that from the e_1-hh$_1$ level. This spreading of the e_1-hh$_1$ excitation into various energy states prior to SPV generation can modify the SPV line shape and account for the difference between the PL and SPV spectra. Also, at low temperatures, increase in the radiative recombination rate (PL generation) actually reduces the SPV generation rate very much, because PL and SPV are two complementary mechanisms. So below ~100 K the e_1-hh$_1$ level effectively broadens as a result of the interaction with the BE level. Above ~100 K, thermalization of carriers prevents the excitation of the BE level and no such broadening in the e_1-hh$_1$-related SPV feature is observed. However, a detailed analysis of the line shape requires further investigation and modeling the various rate processes, which is beyond the scope of the work described here.

V. MECHANISMS OF SPV GENERATION IN A QW STRUCTURE

The SPV of bulk GaAs results from separation of charge carriers in the built-in surface field following carrier generation by photoexcitation. How is the SPV generated when we excite carriers within the QW? In order to produce SPV, separation of carriers is necessary after photogeneration. Three processes of charge separation can be envisaged, as shown schematically in Fig. 7. These are (a) thermal emission of carriers out of the well followed by field separation, (b) tunneling of carriers out of the well followed by field separation, and (c) separation of carriers within the QW itself with possible capture into interface traps. The QW in both samples A and B is situated within the depletion region, which is around 1500 Å thick[44] for n-type doping of $\sim 5 \times 10^{16}\,\mathrm{cm}^{-3}$, whereas the top cap layer of GaAs is 1000 Å thick [See Fig. 8(a)]. It is difficult to distinguish between thermal and field-aided emission processes as such from measurements on samples in which the QW is situated in the

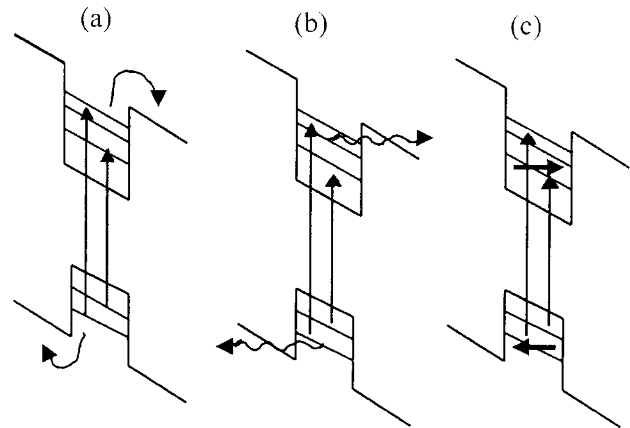

FIG. 7. Possible escape mechanisms for photogenerated carriers out of the quantum well and SPV generation. (a) Thermal emission and carrier separation. (b) Field-aided tunneling emission and carrier separation, and (b) separation of photocarriers within the QW.

depletion region. To distinguish between these processes, instead we select a sample C with the same structure and n-type doping ($\sim 5 \times 10^{16}\,\mathrm{cm}^{-3}$) as samples A and B; however, in this case the top GaAs is thicker (around 3000 Å) such that the QW is located in the neutral region at zero bias [see Fig. 8(b)]. Figure 9 shows a room-temperature $1/C^2$ vs V plot of sample C with a Au-Ge-Ni back Ohmic contact and semitransparent Au top Schottky contact. The onset of the saturation region in Fig. 9 at around 1.2 V negative bias

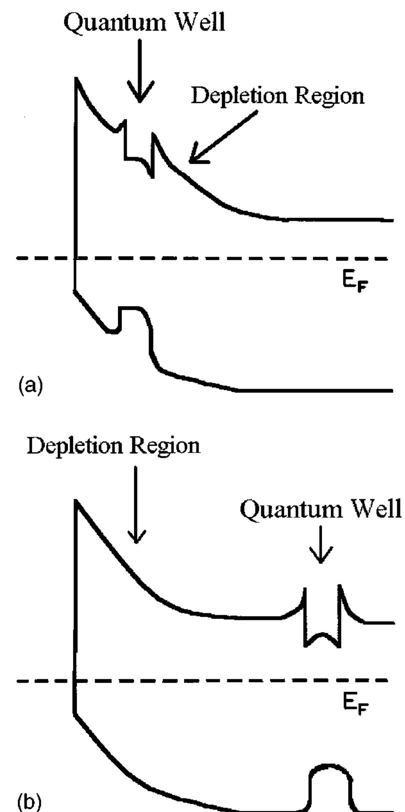

FIG. 8. (a) Schematic band diagram of samples A and B. This also represents the band diagram for sample C under reverse bias (say −2.5 V). (b) Schematic band diagram for sample C under zero bias.

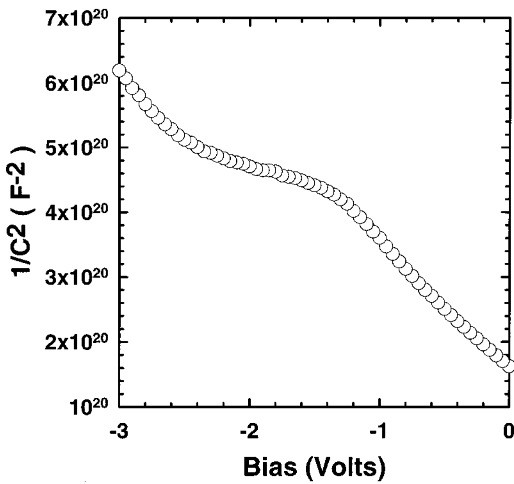

FIG. 9. $1/C^2$ vs bias plot for sample C at room temperature. The QW reaches the depletion edge as the reverse bias is increased, as represented by the saturation region of the plot.

occurs as the depletion region widens and reaches the depth at which the QW is located. Thus at zero bias the QW is well beyond the depletion region. With the application of about −2 V bias, sample C resembles the condition of both samples A and B, where the QW is already within the surface depletion region. Thus, we can alter the field within the QW by varying the reverse bias.

To gain insight into the relative significance of thermal emission, field-aided emission, and charge separation processes, we have carried out measurements of the dc photocurrent as a function of temperature at different reverse bias voltages applied to the top semitransparent Au Schottky contact of sample C. For photoresponse measurements with applied bias, we measure the dc photocurrent versus bias voltage under dark as well as light conditions. The wavelength of the light (950 nm) incident on the semitransparent Au Schottky dot is selected so as to produce a uniform generation rate in the QW over the range of temperatures 289–8.6 K used in these measurements. The photoresponse is obtained from the difference between the current values under illuminated and dark conditions [$\Delta I = I(\text{Illuminated}) - I(\text{dark})$]. Representative results of these measurements are shown in Fig. 10(a). In Fig. 10(b), we have replotted the data of Fig. 10(a) in an Arrhenius plot[45] of ΔI versus $1000/T$ at each bias. The results can be summarized as follows.

From Fig. 10(a) we see that at zero bias the photoresponse decreases by a factor of ~50 as the sample temperature is lowered from 289 to 8.6 K. At larger reverse bias voltages (say, at −2.5 V), the change in the same temperature range is relatively small, about a factor of ~6 only. From this temperature-dependent behavior it is clear that, when the QW of sample C is situated in a field region, field-aided tunneling emission is responsible for the removal of photogenerated carriers from the QW into the barrier region followed by separation in the field region (the same mechanism is also responsible for SPV generation in samples A and B). Since the field-aided tunneling emission is relatively independent of temperature, the change in photocurrent due to cooling of the sample is small, as observed in the relatively flat region in the Arrhenius plots for higher negative biases in Fig. 10(b). As the field in the QW region is reduced, the

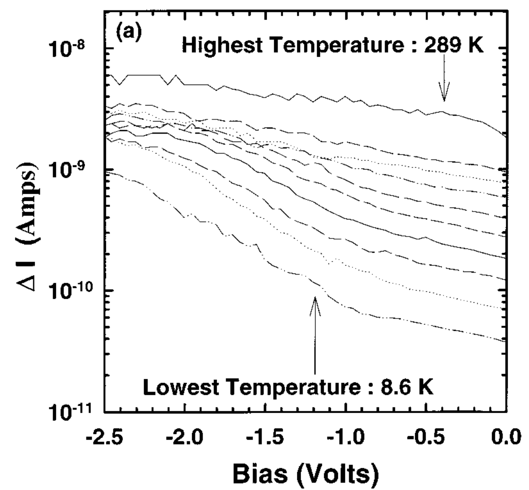

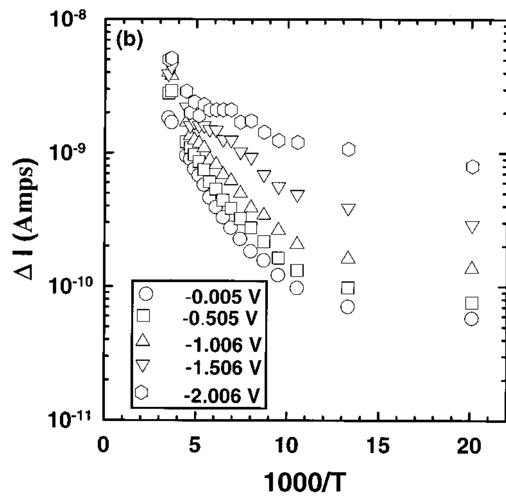

FIG. 10. (a) Photoresponse of sample C under different bias is plotted for various temperatures. Clearly the temperature dependence of ΔI is orders of magnitude larger at zero bias than at −2.5 V bias. (b) Arrhenius plot of the photoresponse as measured on sample C.

field-aided emission strength reduces and the sample has to be cooled to lower temperature before the field-aided emission becomes predominant. The changeover of the emission mechanism occurs at a temperature where the strength of the thermal emission component decreases significantly in comparison. This explains the highest sensitivity of the photoresponse to the sample temperature when the applied bias is zero. Moreover, the existence of dc photocurrent under high reverse bias even at the lowest temperatures used in the experiment clearly shows that the contribution of the third mechanism [as mentioned in Fig. 7(c)] of photogenerated carriers separating within the QW is insignificant in the SPV generation process.

The question may be raised: how does the net photocurrent arise where the QW is located in the neutral region? It is suggested that after thermal emission carriers diffuse in the barrier region and minority carriers reaching the depletion edge constitute the current flow. Accordingly, enhancement of the photocurrent is expected as the depletion edge moves closer to the QW. Within the scheme of carrier escape mechanisms outlined above, it may be expected that at zero bias the photocurrent will continue to decrease monotoni-

cally with lowering of the sample temperature down to the lowest temperature ~8.6 K used in the experiments. Contrary to this, we find that the photocurrent tends to saturate below ~100 K even at zero bias. Although the third mechanism of photogenerated carriers separating within the QW is temperature independent, we exclude this process for reasons mentioned above. Alternatively, we need to assume that the field extends into the well region below 100 K even at zero bias. Support for this is obtained from the measurement of C-V characteristics at low temperatures. We find that the flat region in $1/C^2$-V characteristics extends toward zero bias with lowering of the sample temperature, which could give rise to some field-aided emission, thereby reducing the thermal emission dependence.

The slope of the linear portion of each Arrhenius plots in Fig. 10(b) gives the activation energy of thermal emission of photogenerated carriers within the QW. Measured values of the activation energies range from 75 meV at zero bias to 55 meV at −2 V reverse bias. These activation energy values are much smaller than the values of activation energy of the quenching of PL (~160 meV) as reported above. It is useful to state, however, that the PL measurement is done under Ar^+ ion laser excitation with much larger excitation intensity than the intensity of the light from the quartz-tungsten-halogen lamp used in the SPV and dc photocurrent experiments. From this, we expect the bands to be essentially flat during the PL measurement and the corresponding value of the activation energy for emission of the carriers out of the QW will be higher. Relatively smaller values of the activation energy from the photocurrent measurements can result because of the field lowering of the barrier height of the QW. A detailed modeling will be necessary to confirm this aspect.

VI. CONCLUSIONS

We have reported the temperature dependence of surface photovoltage measurements on a strained GaAs/In_xGa_{1-x}/As/GaAs single quantum well. We have discussed the effect of a bound exciton transition on the broadening parameter (Γ_0) of e_1-hh_1 in SPV spectra below ~100 K. Photoluminescence measurements were performed to explain the unusual broadening of the e_1-hh_1 transition as a result of this bound excitonic transition along with the subband transitions in the quantum well. We have also reported selectively excited dc photocurrent experiments to show that both thermal emission and field-aided tunneling emission of photogenerated carriers from the quantum well are contributing mechanisms for generation of SPV, with field-aided tunneling emission dominating the low-temperature regimes.

ACKNOWLEDGMENTS

The authors wish to thank Professor K. L. Narasimhan and Dr. Sandip Ghosh for their valuable suggestions. S. D. thanks Dr. R. Venkatraghavan, M. R. Gokhale, V. M. Upalekar, and P. B. Joshi for their help.

*Electronic address: shouvik@tifr.res.in

[1] E. O. Johnson, Phys. Rev. **111**, 153 (1958).
[2] Alvin M. Goodman, J. Appl. Phys. **32**, 2550 (1961).
[3] D. R. Frankl and E. A. Ulmer, Surf. Sci. **6**, 115 (1966).
[4] D. L. Lile, Surf. Sci. **34**, 337 (1973).
[5] C. L. Balestra, J. Lagowsi, and H. C. Gatos, Surf. Sci. **64**, 457 (1977).
[6] J. Lagowski, W. Walukiewicz, M. M. G. Slusarczuk, and H. C. Gatos, J. Appl. Phys. **50**, 5059 (1979).
[7] Shailendra Kumar and S. C. Agarwal, Appl. Phys. Lett. **45**, 575 (1984).
[8] W. H. Howland and S. J. Fonash, J. Electrochem. Soc. **142**, 4262 (1995).
[9] Leeor Kronik and Yoram Shapira, Surf. Sci. Rep. **37**, 1 (1999) (review article on SPV).
[10] M. Leibovitch, L. Kronik, E. Fefer, and Yoram Shapira, Phys. Rev. B **50**, 1739 (1994).
[11] Q. Liu, H. E. Ruda, G. M. Chen, and M. Simard-Normandin, J. Appl. Phys. **79**, 7790 (1996).
[12] L. Kronik and Yoram Shapira, J. Vac. Sci. Technol. A **11**, 3081 (1993).
[13] L. Kronik, L. Burstein, Yoram Shapira, and M. Oron, Appl. Phys. Lett. **63**, 60 (1993).
[14] Qiang Liu, Chao Chen, and Harry Ruda, J. Appl. Phys. **74**, 7492 (1993).
[15] L. Kipp, R. Adelung, N. Trares-Wrobel, and M. Skibowski, Appl. Phys. Lett. **74**, 1836 (1999).
[16] Shailendra Kumar, Tapas Ganguli, Pijush Bhattacharya, U. N. Roy, S. S. Chandvankar, and B. M. Arora, Appl. Phys. Lett. **72**, 3020 (1998).
[17] M. Leibovitch, L. Kronik, E. Fefer, V. Korobov, and Yoram Shapira, Appl. Phys. Lett. **66**, 457 (1995).
[18] N. Bachrach-Ashkenasy, L. Kronik, Yoram Shapira, Y. Rosenwaks, M. C. Hanna, M. Leibovitch, and Prakhya Ram, Appl. Phys. Lett. **68**, 879 (1996).
[19] N. Ashkenasy, M. Leibovitch, Yoram Shapira, Fred Pollak, G. T. Burnham, and X. Wang, J. Appl. Phys. **83**, 1146 (1998).
[20] M. Leibovitch, L. Kronik, E. Fefer, L. Burnstein, V. Korobov, and Yoram Shapira, J. Appl. Phys. **79**, 8549 (1996).
[21] Lionel Aigouy, Fred H. Pollak, John Petruzzello, and Khalid Shahzad, Solid State Commun. **102**, 877 (1997).
[22] B. Q. Sun, Z. D. Lu, D. S. Jiang, J. Q. Wu, Z. Y. Xu, Y. Q. Wang, J. N. Wang, and W. K. Ge, Appl. Phys. Lett. **73**, 2657 (1998).
[23] L. Burnstein, Y. Shapira, J. Partee, J. Shinar, Y. Lubianiker, and I. Balberg, Phys. Rev. B **55**, R1930 (1997).
[24] B. O. Seraphin, in *Semiconductors and Semimetals*, edited by R. K. Willardson and Albert C. Beer (Academic, New York, 1972), Vol. 9, p. 1.
[25] D. E. Aspnes, in *Handbook of Semiconductors*, edited by Minko Balakanski (North-Holland, New York, 1980), Vol. 2, p. 109.
[26] X. Yin and Fred H. Pollak, Appl. Phys. Lett. **59**, 2305 (1991). Also see the review article by Fred H. Pollak and H. Shen, Mater. Sci. Eng., R. **10**, 275 (1993).
[27] H. Barry Bebb and E. W. Williams, in *Semiconductors and Semimetals* (Ref. 24), Vol. 8, p. 181.
[28] Shouvik Datta, Sandip Ghosh, and B. M. Arora (unpublished).
[29] D. E. Aspnes, Surf. Sci. **37**, 418 (1973).
[30] D. E. Aspnes and N. Bottka, in *Semiconductors and Semimetals* (Ref. 24), Vol. 9, p. 457.
[31] Y. P. Varshni, Physica (Amsterdam) **34**, 149 (1967).

[32] R. Passler, J. Appl. Phys. **83**, 3356 (1998).
[33] L. Vina, S. Logothetidis, and M. Cardona, Phys. Rev. B **30**, 1979 (1984).
[34] C. D. Thurmond, J. Electrochem. Soc. **122**, 1133 (1975).
[35] A. Manoogian and J. C. Woolly, Can. J. Phys. **62**, 285 (1984).
[36] E. Grilli, M. Guzzi, R. Zamboni, and L. Pavesi, Phys. Rev. B **45**, 1638 (1992).
[37] R. Passler and G. Olegart, J. Appl. Phys. **82**, 2611 (1997).
[38] R. Passler, Phys. Status Solidi B **200**, 155 (1997).
[39] R. Passler, J. Appl. Phys. **88**, 2570 (2000).
[40] Zheng-Yun Wu, Xiao-Jun Wang, and Qi-Sheng Huang, Phys. Status Solidi B **213**, 343 (1999).
[41] D. C. Reynolds, C. E. Leak, K. K. Bajaj, C. E. Stutz, R. L. Jones, K. R. Evans, P. W. Yu, and W. M. Theis, Phys. Rev. B **40**, 6210 (1989).
[42] Hiroyuki Nashiki, Ikuo Suemune, Hideki Suzuki, and Katsuhiro Usegi, Jpn. J. Appl. Phys., Part 1 **36**, 4199 (1997).
[43] S. Weber, W. Limmer, K. Thonke, R. Sauer, K. Panzlaff, G. Bacher, H. P. Meier, and P. Roentgen, Phys. Rev. B **52**, 14 739 (1995).
[44] S. M. Sze, *Physics of Semiconductor Devices*, 2nd ed. (Wiley, New York, 1981), pp. 78–79.
[45] J. Nelson, M. Paxman, K. W. J. Barnham, J. S. Roberts, and C. Button, IEEE J. Quantum Electron. **29**, 1460 (1993).